Rational Design Approach for Integral Abutment Bridge Piles

ROBERT E. ABENDROTH AND LOWELL F. GREIMANN

The piles for an integral abutment bridge are subjected to horizontal movements caused by the expansion and contraction of the bridge superstructure. To design the abutment piles properly, a rational design approach was developed to simplify the complex behavior associated with pile and soil interaction. Fundamental principles for two pile design alternatives that were formulated in a recently completed research study involving experimental and analytical investigations are presented. Alternative 1 was based on elastic behavior and is recommended for piles with limited ductility, such as timber, concrete, and steel sections having insufficient moment-rotation capacity. Alternative 2 was based on inelastic behavior involving plastic redistribution of internal forces caused by the lateral displacement of the pile head and is recommended for piles with adequate moment-rotation capacity at plastic hinge locations. Steel piles do not have to be classified as compact sections to meet the moment-rotation requirement. A ductility criterion, expressed in terms of lateral pile head displacement, is given to evaluate whether the moment-rotation capacity of an HP-shaped pile exceeds the moment rotation demand. To illustrate both design alternatives, a design example for a steel, HP-shaped, friction pile is presented. For the specific example, Alternative 2 is shown to permit the safe design of integral abutment bridges that are substantially longer than those designed according to Alternative 1.

Jointless bridges do not contain traditional expansion joints between the abutments and the bridge superstructure. Instead, the bridge girders and the abutments are connected together forming rigid joints. The piles of the integral abutment are subjected to horizontal movement as the bridge superstructure expands and contracts as a result of seasonal temperature changes. The induced axial and bending stresses in the abutment piles limit the total bridge length. These bridge length limitations vary considerably from state to state because a consistent pile design philosophy has not been established by the state departments of transportation or AASHTO. Recently conducted surveys (*1–4*) have shown that integral abutment bridges have been designed with a variety of specialized details. To establish rational pile design criteria, an experimental and analytical study (*5*) was recently completed. This research involved one-tenth scale laboratory pile tests, full-scale field tests of piles, and finite element investigations using a previously developed analytical model (*2*, *6*) that accounts for nonlinearity of both the soil and pile behavior. The design method summarized in this paper represents a refinement of a method, previously published by Greimann and Wolde-Tinsae (*7*), that incorporates the AASHTO Specification on beam-column design. Equivalent cantilevers replace the actual pile for design purposes. The problem of pile ductility (inelastic hinge rotation capacity) associated with lateral pile head displacements was also not addressed in the Greimann and Wolde-Tinsae paper (*7*).

Two pile design alternatives are presented that address the following three AASHTO Specification design criteria:

- Capacity of the pile as a structural member (Case A);
- Capacity of the pile to transfer the load to the ground (Case B); and
- Capacity of the ground to support the load (Case C).

Alternative 1 is a conventional elastic design approach, whereas Alternative 2 is an inelastic design approach that recognizes redistribution principles, when adequate pile ductility exists. An example is presented for the design of an HP-shaped friction pile to illustrate both design alternatives.

PILES DESIGNED AS BEAM-COLUMNS (AASHTO CASE A)

Equivalent Cantilevers

A pile embedded in soil can be analytically modeled as an equivalent beam-column without transverse loads between the member ends and with a base fixed at a specific soil depth. Either a fixed head or pinned head for the beam-column approximates the actual rotational restraint at the pile head. Figure 1 shows an idealized fixed-headed pile for both an "actual" system and the corresponding equivalent cantilever system. The total length, L, of the equivalent cantilever equals the sum of the length, l_u, above the ground and the length, l_e, from the soil surface to the fixed base of the equivalent cantilever. The three equivalent cantilever lengths (*8*) considered in the development of the design alternatives were the horizontal stiffness of the soil and pile system, the maximum moment in the pile, and the elastic buckling load of the pile. The pile lengths l_e and l_u can be nondimensionalized by the length, l_c, that defines whether the pile behaves as a rigid or flexible pile (*9*). The length l_c is given as

$$l_c = 4\sqrt[4]{EI/k_h} \quad (1)$$

where E is the modulus of elasticity for the pile material, I is the moment of inertia of the pile with respect to the plane of bending, and k_h is the horizontal stiffness of the soil. Greimann, et al. (*5*) developed a nondimensionalized relationship between l_u and l_e for a fixed-headed pile (Figure 2) and for a pinned-headed pile in a uniform soil.

Bridge Engineering Center, Town Engineering Building, Iowa State University, Ames, Iowa 50011.

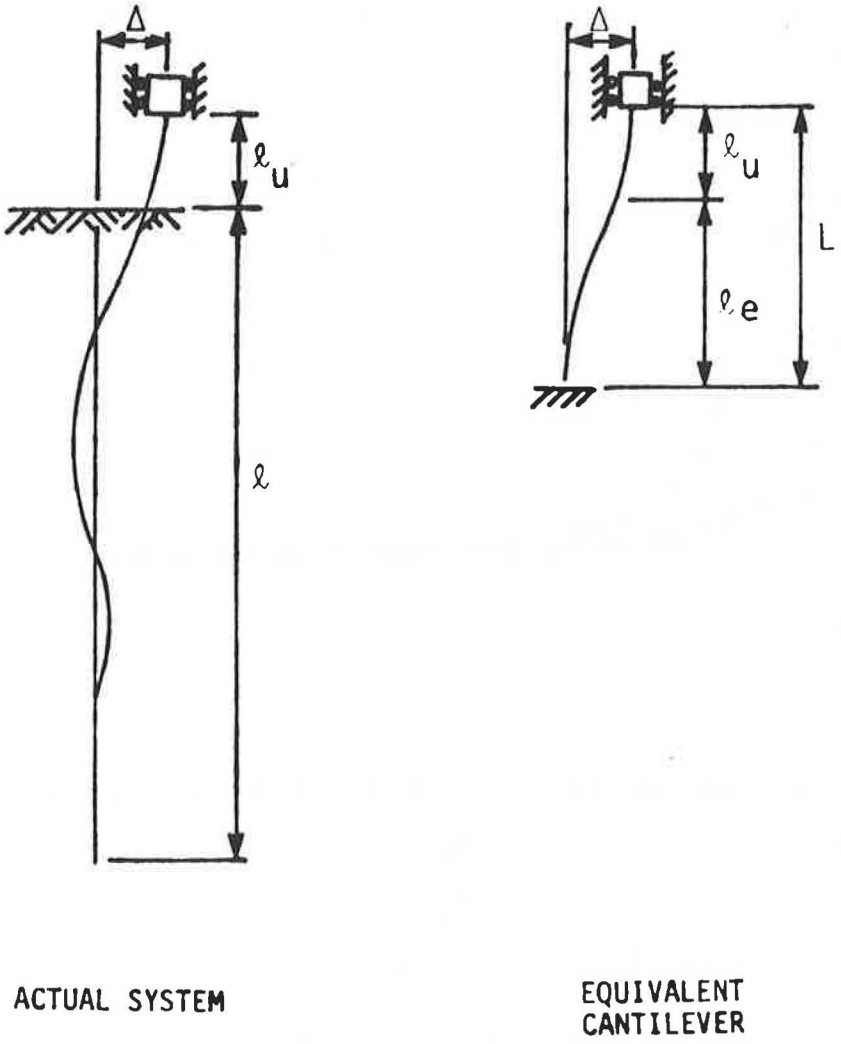

FIGURE 1 Cantilever idealization of a fixed-headed pile.

For nonuniform soil conditions, an equivalent uniform lateral soil stiffness parameter, k_e, is needed to evaluate the length l_c. Figure 3*a* shows the lateral stiffness, k_h, profile for a soil consisting of a sand overlaying a clay layer. The parameter k_{h1} represents the lateral stiffness of the sand at the depth l_1, whereas k_{h2} is the lateral stiffness of the clay soil. To establish k_e, the work done by the actual soil resistance (Figure 3*a*) in moving through the lateral soil displacement (Figure 3*c*) will be equated to the work done by the equivalent soil resistance (Figure 3*b*) in moving through the same soil displacement. Equating the external work expressions for both systems,

$$\int_o^{l_o} \frac{k_h(x)y^2}{2}\,dx = \int_o^{l_o} \frac{k_e\,y^2}{2}\,dx \tag{2}$$

where the length l_o, given by Equation 3, is the active length of the pile in bending, which is taken as one-quarter of the deflected wave shape.

$$l_o = l_c/2 \tag{3}$$

The displaced shape can be approximated by the straight line shown in Figure 3*c*, for which

$$y = \Delta_g\,(1 - \frac{x_1}{l_o}) \tag{4}$$

where Δ_g is the lateral displacement of the pile at the bottom of the abutment and x_1 is the depth below the abutment. Substituting Equation 4 into Equation 2 gives

$$k_e = \frac{3}{l_o^3}\int_o^{l_o} k_h(x)\,(l_o - x_1)^2\,dx \tag{5}$$

The integral expression in Equation 5 is the second moment of the area of the $k_h(x)$ diagram (Figure 3*a*) taken about a line at the depth l_o. Because the length l_o is a function of k_e, an iterative procedure is needed to calculate k_e.

Design Alternatives 1 and 2

Design Alternative 1 is based on elastic pile behavior and neglects the potential reserve strength associated with plastic

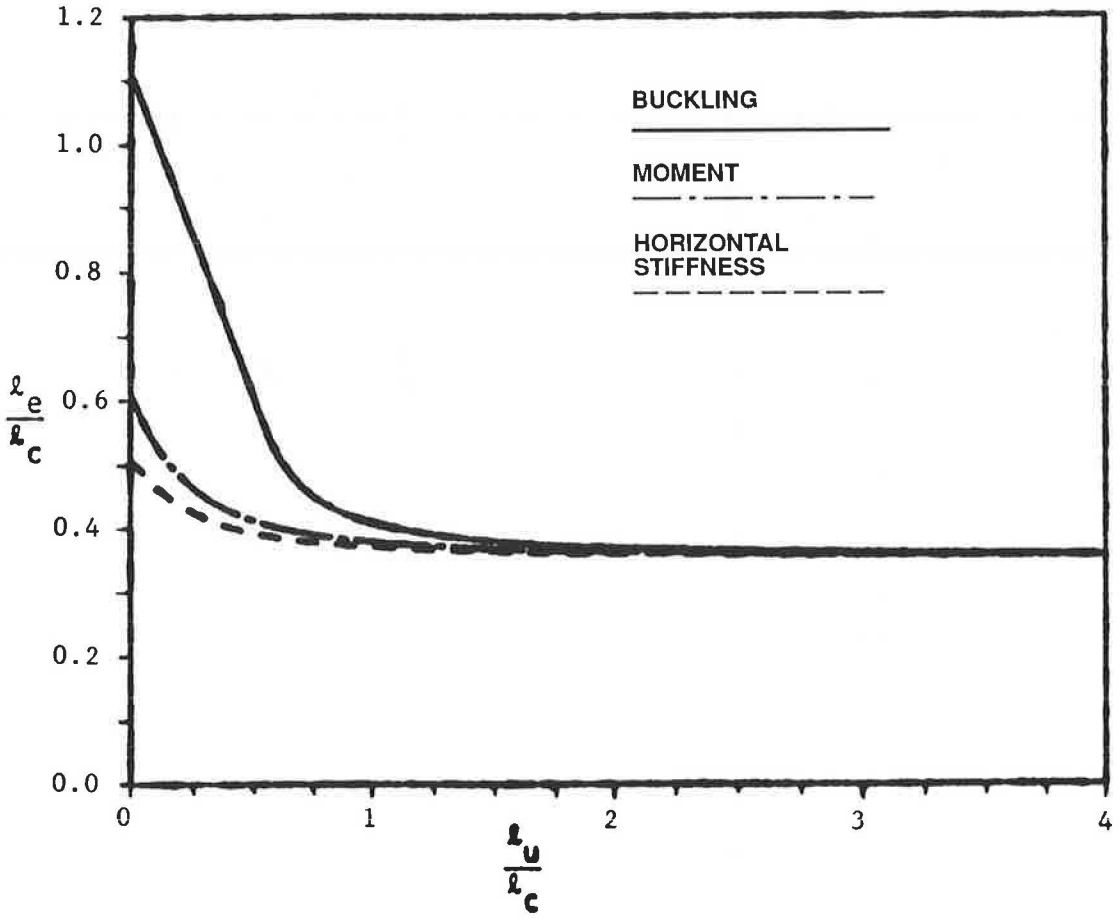

FIGURE 2 Equivalent cantilever for fixed-headed pile in a uniform soil.

hinge formations. Therefore, redistribution of internal forces is not permitted to occur for ultimate strength. This design method is a conventional elastic design procedure for the equivalent cantilever (beam-column) that considers all stresses developed in the pile. The lateral displacement, Δ, at the pile head, caused by expansion and contraction of the bridge superstructure, induces a first-order elastic end moment, M, given by

$$M = \frac{D_1 EI\Delta}{L^2} \tag{6}$$

where the bending moment coefficient D_1 equals 6 or 3 for fixed-headed or pinned-headed piles, respectively. This moment can be anticipated to dramatically affect the pile capacity.

Design Alternative 2 accounts for the redistribution of forces associated with plastic hinge formations in the pile as a result of lateral displacement of the pile head. The stresses induced by the horizontal pile head movement are considered not to significantly affect the pile ultimate strength, as long as the corresponding strains can be accommodated through adequate pile ductility. Neglecting these thermally induced pile stresses is justified by first-order plastic theory involving small displacements. According to this theory, the plastic collapse load is not affected by residual stresses, thermal stresses, imperfect fit, or, in this case, support movement (*10*,*11*), as long as local and lateral buckling are prevented.

For Alternative 2, the axial pile load, P, produces a second-order bending moment as a result of the lateral displacement at the pile head. A conservative upper bound on this induced end moment is

$$M = D_2 P\Delta \tag{7}$$

where the bending moment coefficient D_2 equals one-half or unity for fixed-headed or pinned-headed piles, respectively.

During the development of the design alternatives, comparisons were made of ultimate strength predicted by both alternatives and the experimentally verified finite element solution (*5*). Local and lateral buckling were not considered, because the finite element analysis did not model this type of behavior. For an HP 10 x 42 pile, the results showed that both design alternatives were conservative, considering practical ranges of sand density, clay stiffness, and column slenderness. Alternative 1 was excessively conservative for small slenderness ratios where yielding controls over stability. The design alternatives and the finite element model predicted a decrease in the ultimate pile capacity with increasing horizontal head movement.

Ductility Conditions

Both design alternatives must satisfy local buckling criteria that are not as stringent as those given in Article 10.48.1 of

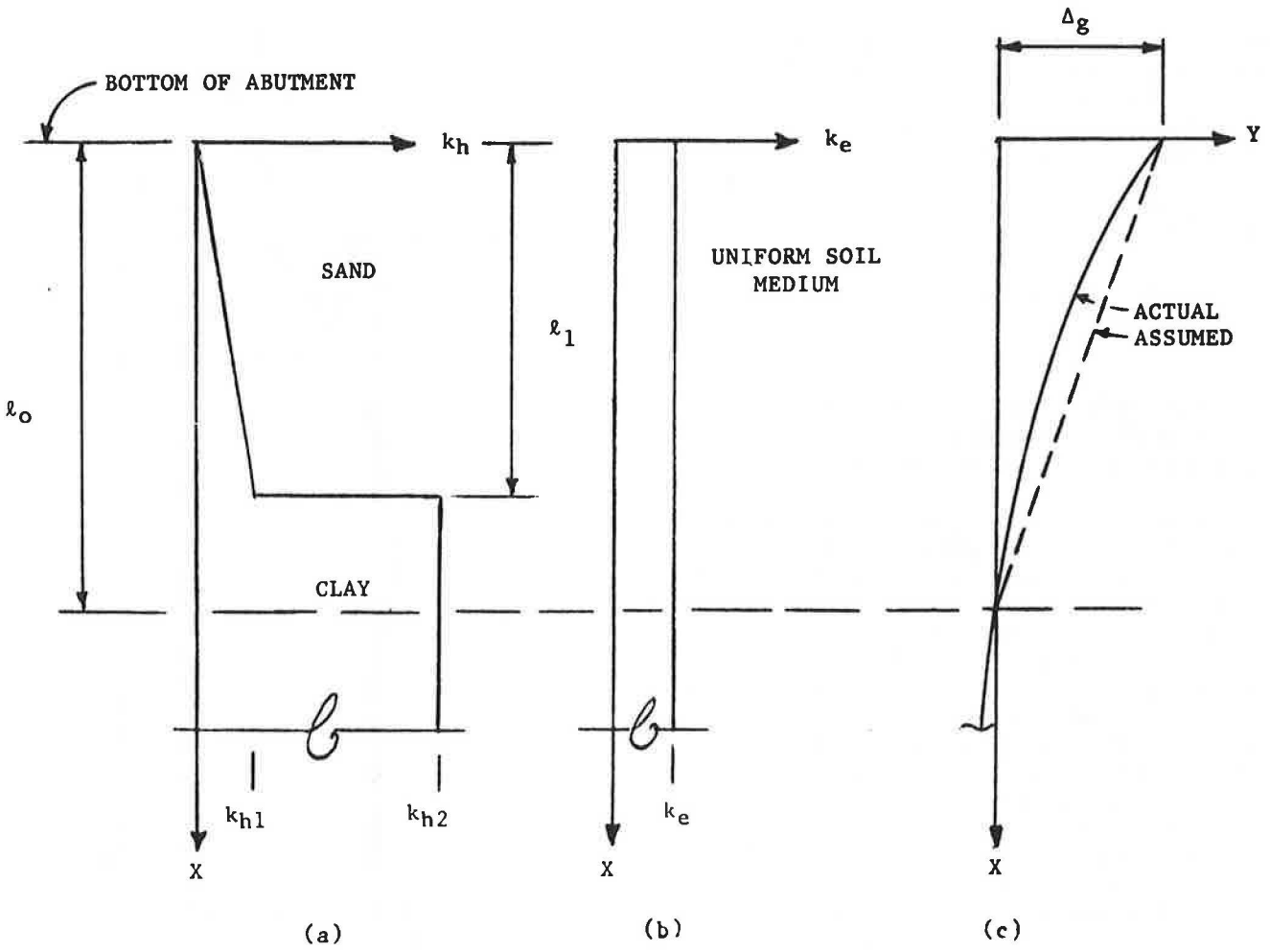

FIGURE 3 Horizontal soil stiffness and displacement: (*a*) actual soil, (*b*) equivalent soil, and (*c*) displaced shape.

the AASHTO Specification. For Alternative 1, the width-to-thickness ratios of the cross-sectional elements must be limited to prevent local buckling before the yield moment is obtained. Applying Article 1.9 of the American Institute of Steel Construction (AISC) Specification (*12*), the standard rolled HP shapes satisfy these width-thickness criteria; therefore, local buckling will not govern the pile capacity for this design alternative.

Alternative 2 requires additional ductility beyond that needed for Alternative 1 in order to develop the inelastic rotation capacity associated with plastic hinge formations. To provide the necessary inelastic rotation capacity, the flange width-to-thickness ratio must be limited to prevent local buckling for the total range of horizontal pile head movement. Based on studies of moment-rotation relationships for strong-axis bending of I-shapes (*13–16*) Greimann et al. (*5*) developed the following ductility criterion that requires that the moment-rotation demand does not exceed the moment-rotation capacity.

$$2\left[\frac{\Delta}{L} - \frac{M_p L}{6EI}\right] + \theta_w \leq \frac{3C_i M_p L}{4EI} \tag{8}$$

where M_p is the plastic moment capacity of the pile, θ_w is the pile head rotation caused by the bridge girder end rotation induced by gravity loads applied after the girder and abutment become monolithic, and C_i is an inelastic rotation capacity reduction factor, based on the flange width-to-thickness ratio. The expression for C_i is

$$C_i = \frac{19}{6} - \frac{b_f\sqrt{F_y}}{60\,t_f} \tag{9}$$

where b_f and t_f are the flange width and thickness, respectively, and F_y is the yield strength. An upper bound of unity for C_i applies when $b_f/2t_f \leq 65/\sqrt{F_y}$, and a lower bound of zero governs when $b_f/2t_f \geq 95/\sqrt{F_y}$. These limits correspond to an inelastic rotation capacity of 3 and 0 (*17*), respectively. Incorporating a factor of safety equal to F_y/F_b, the ductility criterion (Equation 8), rewritten in terms of the lateral displacement of the pile head, is

$$\Delta \leq \Delta_i \tag{10}$$

with

$$\Delta_i = \Delta_b\,(D_3 + 2.25\,C_i) \tag{11}$$

where Δ_i is the allowable displacement capacity of the pile head, D_3 is a ductility coefficient equal to 0.6 or 1.0 for fixed-headed or pinned-headed piles, respectively, and Δ_b is the horizontal movement of the pile head when the actual extreme fiber bending stress equals the allowable bending stress, F_b. The displacement Δ_b is given as

$$\Delta_b = \frac{F_b S L^2}{D_1 E I} \tag{12}$$

where S is the section modulus of the pile with respect to the plane of bending.

LATERAL DISPLACEMENT EFFECTS ON VERTICAL LOAD TRANSFER AND SOIL STRENGTH (AASHTO CASES B AND C)

Lateral displacement of the pile, shown in Figure 4, can affect the capacity of the pile to transfer load to the ground (Case B) through vertical friction along the embedment length, l, but should not affect the end bearing resistance of flexible piles ($l \geq l_c$), nor the capacity of the ground to support the load (Case C). Fleming, et al. (*18*) have suggested that the displacement y_{max}, representing the maximum lateral displacement below which the frictional resistance is assumed to be unaffected by the movement, be established as 2 percent of the pile diameter. The lengths l_n and l' are the lengths along the pile for which the vertical frictional resistance is assumed to be nonexistent and fully effective, respectively. The effect of the pile length, l_u, above the ground on the length l_n is shown in the nondimensionalized graph of Figure 5 for fixed-headed piles embedded in a uniform soil (or equivalent uniform soil medium). A similar figure has been developed for pinned-headed piles (*5*).

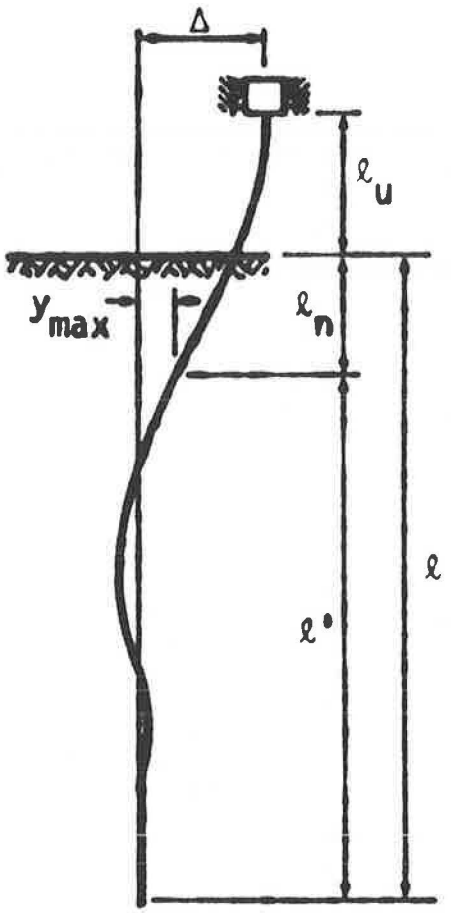

FIGURE 4 Soil-pile system for determining the friction capacity of the pile.

FRICTION PILE DESIGN EXAMPLE

To illustrate the design procedure for both Alternatives 1 and 2, a friction pile will be designed to support a vertical load, P_w, equal to 50 kips, involving dead plus live plus impact loads ($D + L + I$), for the conditions shown in Figure 6. The pile is an HP 10 × 42 with a yield strength, F_y, of 36 ksi. The abutment is supported by eight piles, as shown in Figure 7. The piles were driven in an 8-ft-deep, 2-ft-diameter, predrilled hole that is filled with loose sand. The existing soil consists of an initial 12 ft of stiff clay underlain by very stiff clay. The integral abutment bridge has seven lines of AASHTO Type III bridge girders and five spans having a total length of 360 ft. The end spans are 60 ft long.

SOLUTION

Preliminary Design

The estimated allowable frictional resistance for each steel pile will be taken as 0.8 tons per ft and 1.2 tons per ft for the stiff and very stiff clay, respectively. These values correspond to "firm silty clay" and "firm-very firm glacial clay" in the Iowa Department of Transportation (Iowa DOT) Foundation Soil Information Chart, revised June 1976. Assuming that the capacity of the pile to transfer the load to the ground (Case B) and AASHTO Group I loading controls and neglecting the sand in the predrilled hole, the length of the embedment, l_2, into the very stiff clay is

$$l_2 = \frac{(0.5)(50) - (0.8)(8)}{1.2} = 16 \text{ ft} \tag{13}$$

Equivalent Uniform Soil Stiffness

The lateral soil stiffness, k_h, for the soil in the predrilled hole is not as flexible as a loose sand because the predrilled hole has only a 2-ft diameter and the zone of influence of the pile is approximately six pile diameters or about 5 ft. Therefore, the stiffness will be assumed to correspond to that for loose-to-medium-dense sand. For loose-and-medium-dense sands, the values of k_h, obtained from Table 1 (*5*, excerpt from Table 2.5), are $8.0x$ and $27.0x$ ksf, respectively, where x is the depth in feet at which k_h is evaluated. For a loose-to-medium sand, k_h will be assumed to be equal to $17.5x$ ksf. The lateral stiffness of the soil below the predrilled hole corresponds to that for a stiff clay, for which k_h equals the smaller value of 580 or $(190 + 41x)$ ksf, obtained from Table 1 (*5*, excerpt from Table 2.4). For the sand in the predrilled hole and the stiff clay layer, Figure 3*a* shows the variation in k_h with depth, when

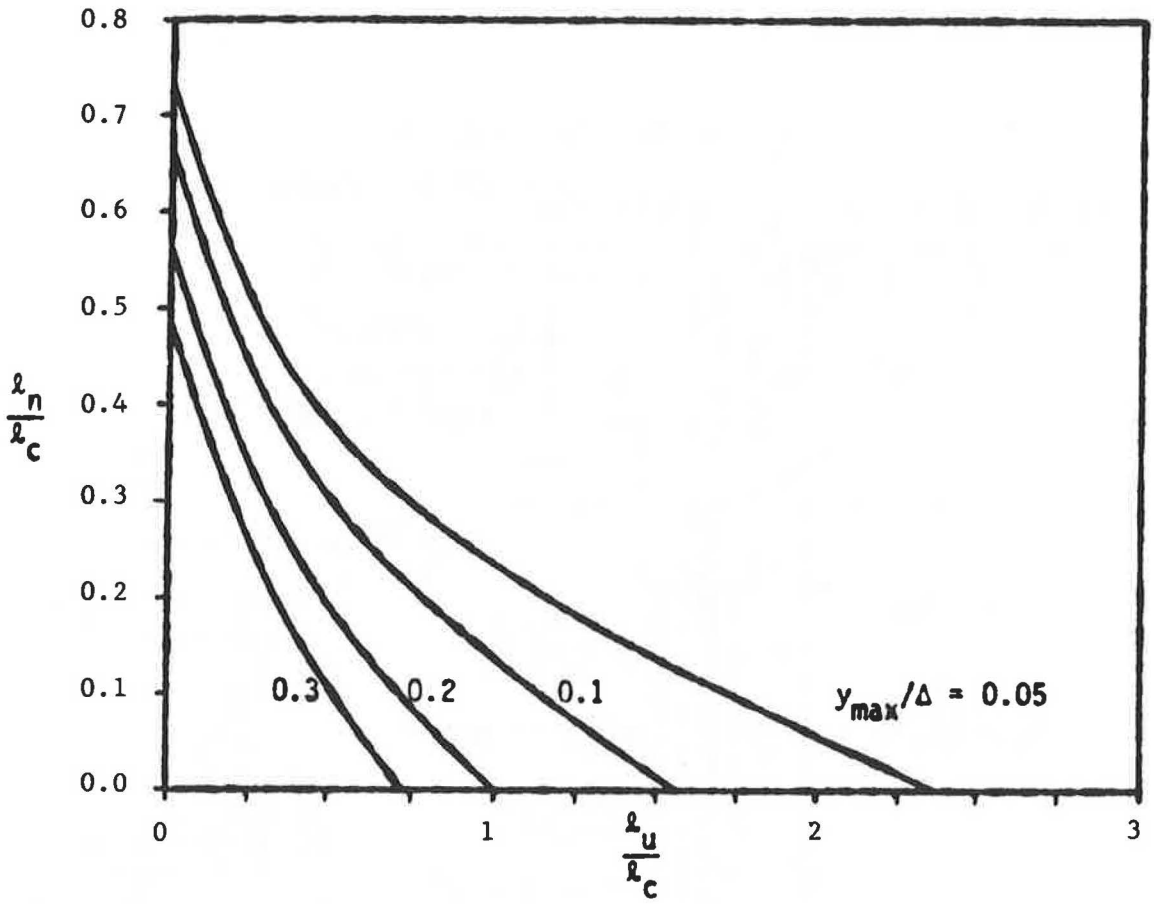

FIGURE 5 Displacement for a fixed-headed pile embedded in a uniform soil.

k_{h1} and k_{h2} equal 140 and 580 ksf, respectively, and l_1 equals 8 ft. The solution for the equivalent uniform soil stiffness, k_e, (Figure 3*b*) converged to 38.8 ksf after two iterations involving Equations 1 through 5. Using k_e as the lateral soil stiffness, k_h, in Equation 1, the length parameter l_c is

$$l_c = \sqrt[4]{\frac{2.08 \times 10^6}{(38.8)\ (144)}} = 17.6 \text{ ft} \tag{14}$$

Equivalent Cantilever Lengths

Assuming the pile head is fixed against rotation (verified later) and taking l_u/l_c equal to 0, the equivalent embedment lengths, l_e, for stiffness, moment, and buckling, obtained from Figure 2, are

$$\begin{aligned} l_e &= 0.5\ l_c = 0.5\ (17.6) \\ &= 8.8 \text{ ft} \quad \text{stiffness} \\ l_e &= 0.6\ l_c = 0.6\ (17.6) \\ &= 10.6 \text{ ft} \quad \text{moment} \\ l_e &= 1.1\ l_c = 1.1\ (17.6) \\ &= 19.4 \text{ ft} \quad \text{buckling} \end{aligned} \tag{15}$$

Because l_u equals 0, the total equivalent cantilever length, L, equals l_e. Now, if the loose sand in the predrilled hole is completely neglected, the critical length, l_c, is 8.9 ft, based on the soil stiffness in the stiff clay of 580 ksf. From Figure 2, with l_u/l_c equal to 8 ft/8.9 ft or 0.9, the equivalent embedded length, l_e, of 3.6 ft is about the same for stiffness, moment, and buckling. The total equivalent cantilever length, L (equal to l_u plus l_e), would become 11.6 ft. The equivalent cantilever for the pile in loose sand should not be reasonably longer than this value. Therefore, the following total equivalent lengths will be used for design:

$$\begin{aligned} L &= 8.8 \text{ ft or } 106 \text{ in.} \quad \text{stiffness} \\ L &= 10.6 \text{ ft or } 127 \text{ in.} \quad \text{moment} \\ L &= 11.6 \text{ ft or } 139 \text{ in.} \quad \text{buckling} \end{aligned} \tag{16}$$

Structural Analysis of Bridge Pile Soil System for Gravity Loads

For simplicity, an approximate structural analysis will be presented to obtain the gravity load moment in the pile for this example. An idealized structural model is shown in Figure 8. Because the composite bending stiffness of the seven girders is at least 100 times the bending stiffness of the eight piles and because the girder continuity at the first pier can be

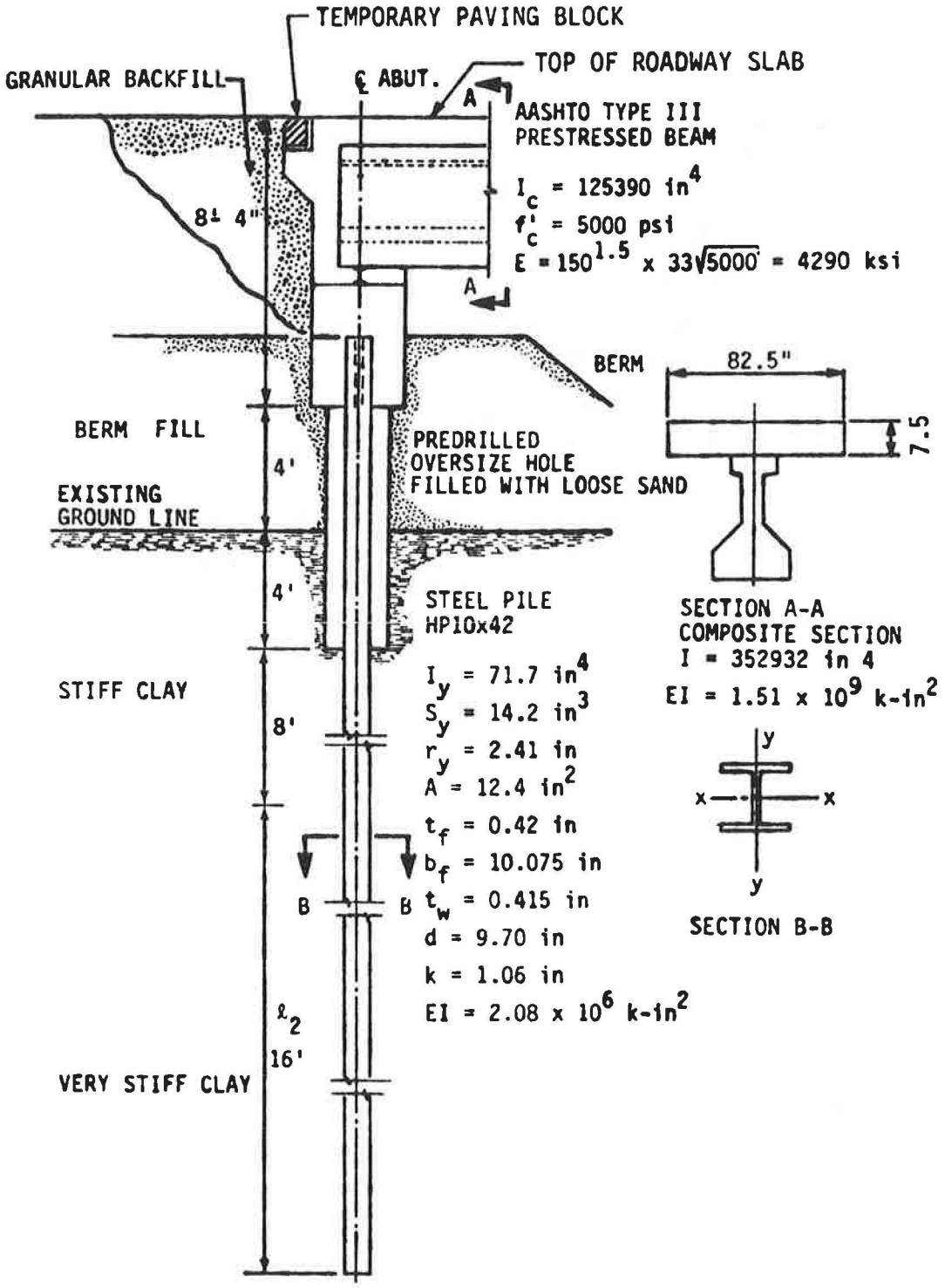

FIGURE 6 Section through abutment and soil profile.

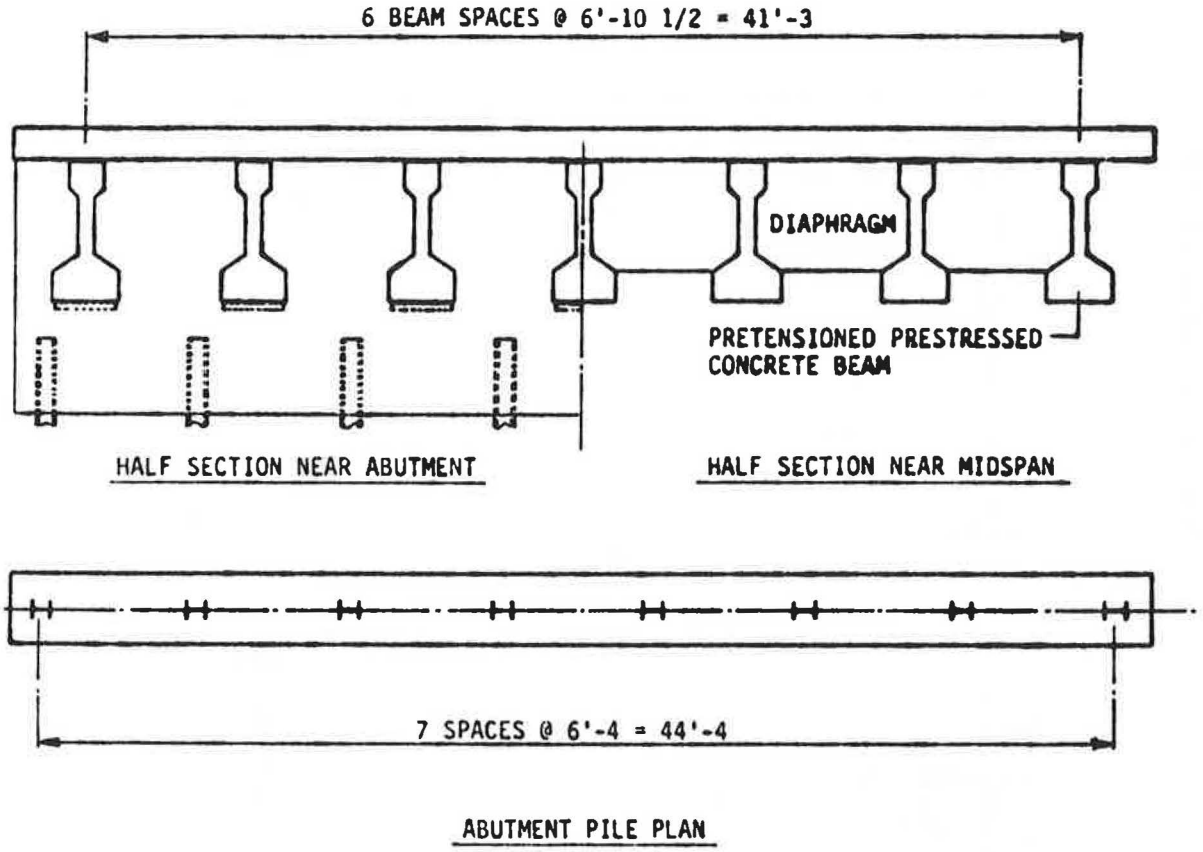

FIGURE 7 Transverse section through bridge and abutment plan.

TABLE 1 LATERAL SOIL STIFFNESS PARAMETER k_h

	k_h (ksf)
Sand	
Loose	$8x$
Medium	$27x$
Dense	$72x$
Clay	
Soft	$(24 + 5.8x) \leq 72$
Stiff	$(190 + 41x) \leq 580$
Very stiff	$(750 + 610x) \leq 2{,}200$

conservatively neglected when the joint rotation at the abutment is being considered, the totals of the uniformly distributed girder load, W, and the corresponding end rotation, θ_w, for the 50-kip pile load $(D + L + I)$ are

$$W = \frac{8\ (50)2}{7} = 114 \text{ kips} \tag{17}$$

$$\theta_w = \frac{WL_g^2}{24\ E_g I_g} = \frac{(114)(60)^2(12)^2}{24(4290)(352{,}932)} = 0.00163 \text{ rad} \tag{18}$$

where L_g, E_g, and I_g represent the length, modulus of elasticity, and moment of inertia, respectively, for an end span bridge girder. Since the top of the pile is rigidly connected to the integral abutment, the pile head will rotate by θ_w. This amount of rotation is an upper bound because the girder and abutment are not monolithic for the total load. Therefore, an upper bound on the induced elastic moment, M_w, in the equivalent cantilever as a result of vertical load is

$$M_w = \left[\frac{4\ EI}{L}\right] \theta_w = \left[\frac{4(29000)(71.7)}{(10.6)\ (12)}\right] (0.00163) = 107 \text{ k-in.} \tag{19}$$

where the equivalent cantilever length, L, for moment (Equation 16) was used.

Structural Analysis for Thermal Expansion

Again, an approximate analysis will be presented for simplicity. The horizontal displacement, Δ, at each abutment, neglecting lateral pier stiffnesses and passive soil pressure against the abutment backwalls, is given by

$$\Delta = 1/2\ \alpha\ \Delta T_{ave}\ L_b \tag{20}$$

where the bridge length, L_b, equals 360 ft and the coefficient of thermal expansion, α, for the concrete superstructure equals 0.000006/°F. Assuming that the bridge is constructed in the middle of an 80°F temperature range, the horizontal displacement at each abutment evaluated from Equation 20 is

$$\Delta = 1/2\ (0.000006)(40)(360)(12) = 0.52 \text{ in.} \tag{21}$$

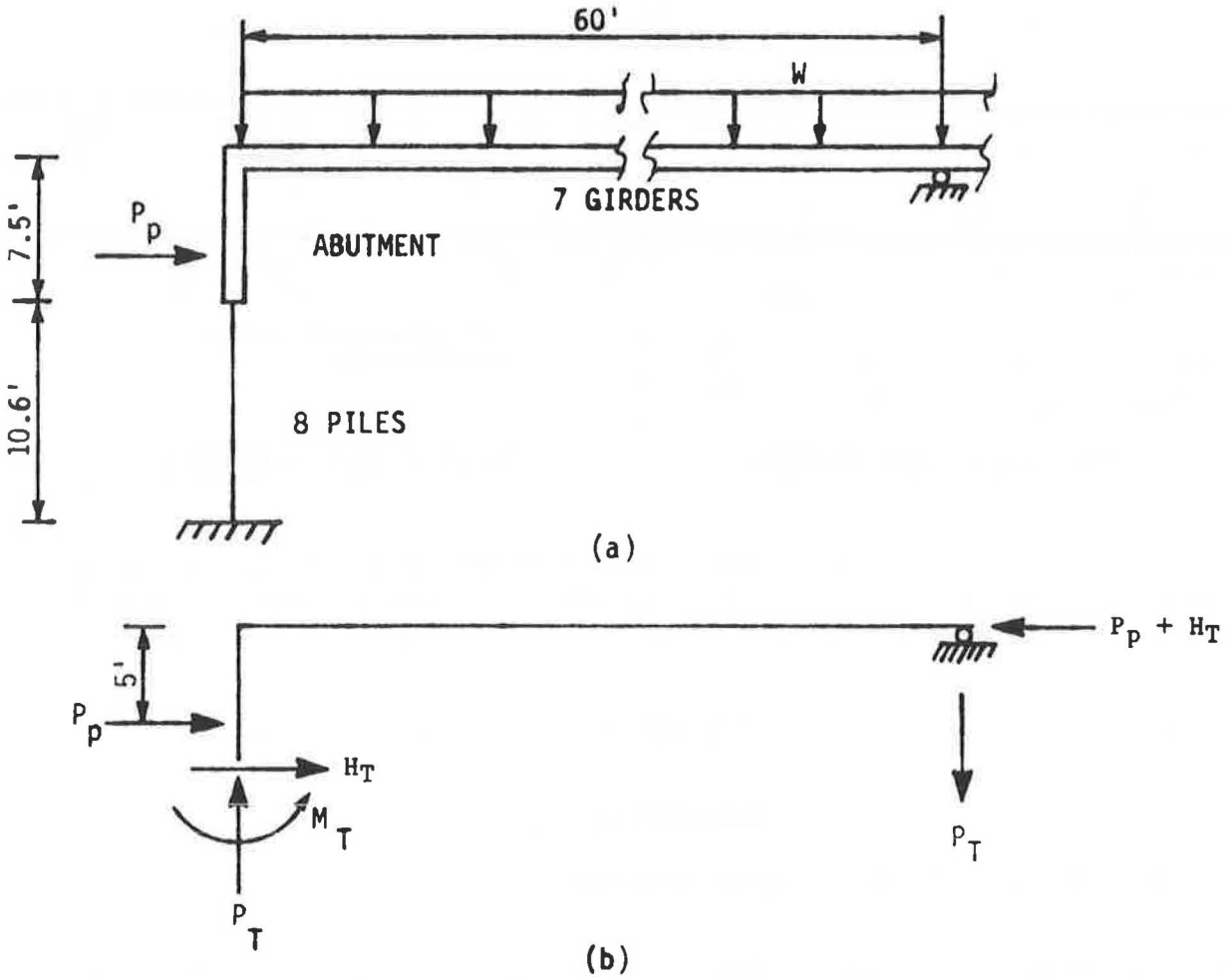

FIGURE 8 Idealized abutment foundation and girder end span: (*a*) structural model and (*b*) free body diagram.

The pile moment, M_T, (Equation 6) and corresponding horizontal force, H_T, induced by this lateral displacement are

$$M_T = \frac{6EI\Delta}{L^2} = \frac{6(29000)(71.7)(0.52)}{(127)^2} = 402 \text{ k-in.} \quad (22)$$

$$H_T = \frac{12EI\Delta}{L^3} = \frac{12(29000)(71.7)(0.52)}{(106)^3} = 10.9 \text{ kips} \quad (23)$$

where the respective equivalent cantilever lengths for the moment and the horizontal stiffness (Equation 16) have been used. (Note that M_T cannot exceed 785 k-in., which is the plastic moment capacity of the pile, and H_T cannot exceed 14.8 kips, which is the shear force associated with a plastic mechanism when L equals 106 in.)

A horizontal force on the back side of the abutment occurs as the bridge expands. This force can be estimated conservatively as the passive resistance of the soil behind the abutment, P_p. Using an elementary soil model for a granular backfill material (*19*),

$$P_p = \frac{1}{2}\gamma h^2 \left[\frac{1 + \sin\phi}{1 - \sin\phi}\right] \quad (24)$$

where γ is the unit soil weight, h is the abutment height, and ϕ is the soil friction angle. Assuming that the granular backfill weighs 130 pcf and has an angle of internal friction equal to 35 degrees, the passive soil pressure along an abutment length equal to the pile spacing of 6.33 ft is

$$P_p = \frac{1}{2}(130)(7.5)^2 \left[\frac{1 + \sin 35°}{1 - \sin 35°}\right](6.33) = 85.4 \text{ kips} \quad (25)$$

Considering equilibrium of a simply supported girder end span shown in Figure 8*b*, thermal expansion of the superstructure induces an axial force in the pile, P_T, given by

$$P_T = \frac{P_P(5.0) + H_T(7.5) + M_T}{60} \quad (26)$$

Substituting values for M_T, H_T, and P_P from Equations 22, 23, and 25, respectively, into Equation 26, the thermally induced axial compression force in the pile is 9.04 kips.

Allowable Axial Stresses

Even though horizontal movement at the top of the abutment pile was caused by the expansion or contraction of the bridge

superstructure, further lateral displacement at the pile head induced by gravity loads is prevented. Therefore, the top of the equivalent cantilever is considered braced against the sidesway. At the head of the equivalent cantilever, the ratio, G, of the flexural stiffness ($4EI/L$) for the eight piles to the flexural stiffness ($3E_gI_g/L_g$) for the seven bridge girders is

$$G = \frac{4[(2.08 \times 10^6)/127](8)}{3[(1.51 \times 10^9)/720](7)} = 0.012 \quad (27)$$

where the length of the equivalent cantilever length, L, for moment (Equation 16) was used. Because the base of the equivalent cantilever is theoretically fixed by definition ($G = 0$), the equivalent cantilever is essentially fixed at both ends, resulting in an effective length factor, K, equal to 0.5. The value of K is increased to 0.65 for design (AASHTO Specification, Table C-1). (Note that the assumption of a fixed-headed pile used in determining l_e and used in the approximate structural analyses was valid.)

The allowable axial stress, F_a, is based on the following governing slenderness ratio:

$$\frac{KL}{r_y} = \frac{(0.65)(139)}{2.41} = 37.5 \quad (28)$$

where the equivalent cantilever length, L, for buckling (Equation 16) was used. Now, following AASHTO Specification, Table 10.32.1A, C_c, the slenderness ratio at the transition point between inelastic and elastic buckling, equals 126.1, which is greater than the governing slenderness ratio of 37.5; therefore, the allowable axial stress is

$$F_a = \frac{36}{2.12}\left[1 - \frac{(37.5)^2(36)}{4\pi^2(29000)}\right] 1.25 = 20.3 \text{ ksi} \quad (29)$$

where the 1.25 factor represents the allowable stress increase for AASHTO Group IV loading obtained from the AASHTO Specification, Table 3.22.1A. The elastic buckling stress, $F_{e'}$, with respect to the plane of bending, including a factor of safety (AASHTO Specification, Equation 10-43) and an allowable stress increase for Group IV loading, is

$$F_{e'} = \frac{\pi^2(29000)(1.25)}{(37.5)^2(2.12)} = 120.0 \text{ ksi} \quad (30)$$

Allowable Bending Stress

Table 10.32.1A of the AASHTO Specification lists an allowable bending stress of 0.55 F_y. No mention is made specifically of weak axis bending or local buckling of the flange. Applying the flange width-to-thickness design criteria in the AISC Allowable Stress Design Specification (*12*), Article 1.5.1.4.1, modified by the ratio of the maximum permissible strong-axis bending stresses in the AASHTO and AISC Specifications (0.55 F_y/0.66 F_y), the following allowable weak-axis bending stresses, F_b, were developed:

$$F_b = \left[\frac{0.55}{0.66}\right](0.75\ F_y) = 0.625\ F_y \quad (31)$$

where

$$\frac{b_f}{2t_f} \le \frac{65}{\sqrt{F_y}}$$

and, by AISC Specification, Equation 1.5–5b,

$$F_b = F_y\left[0.896 - 0.0042\frac{b_f}{2t_f}\sqrt{F_y}\right] \quad (32)$$

where

$$\frac{65}{\sqrt{F_y}} \le \frac{b_f}{2t_f} \le \frac{95}{\sqrt{F_y}}$$

(Note that rather than using Equation 31 for the allowable bending stress, a conservative interpretation of the AASHTO Specification would be to use F_b equal to 0.55 F_y for both strong- and weak-axis bending. However, when local buckling governs the allowable bending stress, using 0.55 F_y for F_b instead of Equation 32 can be unconservative, depending on the magnitude of the width-thickness ratio.) Comparing the flange width-to-thickness proportions for an HP 10 × 42 pile (F_y = 36 ksi) with the two limits,

$$\frac{65}{\sqrt{F_y}} = 10.83 < \frac{b_f}{2t_f} = \frac{10.075}{2(0.420)} = 12.0 < \frac{95}{\sqrt{F_y}} = 15.8 \quad (33)$$

reveals that the HP 10 × 42 shape is "partially compact" with respect to the flange (*12*). Applying Equation 32 and including the allowable stress increase permitted for AASHTO Group IV loading, the allowable bending stress is

$$F_b = 36\left[0.896 - 0.0042(12.0)\sqrt{36}\right](1.25) = 26.7 \text{ ksi} \quad (34)$$

(Note that lateral bracing is not required, because bending occurs about the weak axis (*12*), Commentary Article 1.5.1.4).

Applied Axial Stress

The axial stress, f_a, at the pile head for both Alternatives 1 and 2, resulting from the axial forces from the vertical load and thermal expansion (Equation 26), is

$$f_a = \frac{P_w + P_T}{A} = \frac{50 + 9.04}{12.4} = 4.76 \text{ ksi} \quad (35)$$

Alternative 1 Applied Bending Stress

The extreme fiber flexural stress, f_b, at the pile head for Alternative 1, resulting from the moments due to vertical load (Equation 19) and thermal expansion (Equation 22), is

$$f_b = \frac{M_w + M_T}{S} = \frac{107 + 402}{14.2} = 35.8 \text{ ksi} < F_y = 36 \text{ ksi} \quad (36)$$

Alternative 1 Stability and Strength Interaction Criteria

For the equivalent fixed-ended beam-column, the moment gradient factor, C_m, equals 0.40. However, because the real pile is subjected to transverse loads (soil pressures), C_m can be conservatively taken as 0.85 (*12*, Commentary Article 1.6.1). Substituting the appropriate terms into AASHTO Equations 10-41 and 10-42, including the 25 percent allowable axial stress increase for Group IV loading,

$$\frac{4.76}{20.3} + \frac{0.85(35.8)}{[1 - (4.76/120.0)](26.7)} = 1.42 > 1 \quad (37)$$

$$\frac{4.76}{0.472(36)(1.25)} + \frac{35.8}{26.7} = 1.546 > 1 \quad (38)$$

As expected, stability and strength are not adequate, because f_b is greater than F_b. Therefore, according to Alternative 1, HP 10 × 42 piles cannot be used to support the integral abutment for this bridge example.

Alternative 2 Applied Bending Stress

The moment at the pile head for Alternative 2 is due to vertical load only (Equation 19 plus Equation 7), because Alternative 2 allows for redistribution of forces through inelastic rotation. Therefore, the stresses induced in the pile by the horizontal motion of the pile head are neglected. The moment, M, and corresponding extreme fiber flexural stress, f_b, at the pile head are

$$M = M_w + \frac{P\Delta}{2} = 107 + \frac{(59)(0.52)}{2} = 122 \text{ k-in.} \quad (39)$$

$$f_b = \frac{M}{S} = \frac{122}{14.2} = 8.59 \text{ ksi} \quad (40)$$

Alternative 2 Stability and Strength Interaction Criteria

The stability and strength conditions (AASHTO Equations 10-41 and 10-42) for Alternative 2 are

$$\frac{4.76}{20.3} + \frac{0.85(8.59)}{[1 - (4.76/120.0)](26.7)} = 0.52 < 1 \quad (41)$$

$$\frac{4.76}{0.472(36)(1.25)} + \frac{8.59}{26.7} = 0.55 < 1 \quad (42)$$

Therefore, both stability and strength are adequate for this design alternative.

Alternative 2 Ductility Criterion

Alternative 2 requires sufficient plastic hinge rotation capacity of the pile. For the HP 10 × 42 equivalent cantilever in this example, the inelastic rotation capacity reduction factor given by Equation 9 and the lateral displacement Δ_b, corresponding to the allowable bending stress (Equation 12), are

$$C_i = \frac{19}{6} - \frac{10.075\sqrt{36}}{60(0.420)} = 0.77 \quad (43)$$

$$\Delta_b = \frac{(26.7)(14.2)^3(127)^2}{6(2.08 \times 10^6)} = 0.49 \text{ in.} \quad (44)$$

Substituting the values for C_i and Δ_b into Equation 11, the allowable horizontal displacement capacity, Δ_i, of the pile head is

$$\Delta_i = 0.49\,[0.6 + 2.25\,(0.77)] = 1.14 \text{ in.} \quad (45)$$

Because the lateral displacement demand, Δ, of the pile head resulting from thermal expansion (Equation 21) is only 0.52 in., the HP 10 × 42 pile has more than sufficient ductility for this example.

Induced Girder Forces

The lateral displacement of the fixed-headed abutment piling will induce an additional axial force, P_g, shear force, V_g, and bending moment, M_g, into the bridge girders (Figure 8*b*). These forces are reversible, based on the direction of lateral displacement, and must be considered in the girder design and in the design of the connection between each girder and the abutment. For the simplified example presented, the forces P_g, V_g, and M_g, obtained from Equations 19, 22, 23, 25, and 26, are equal to 110 kips, 10.3 kips, and 582 k-in., respectively, for both Alternatives 1 and 2.

Case B Capacity

The effect of the horizontal displacement on the capacity of the pile to transfer the load to the ground (Case B) must be checked. For the HP 10 × 42 pile, the maximum lateral displacement, y_{max}, below which the frictional capacity is unaffected, is approximately 0.2 in. (2 percent of the 10-in. pile dimension in the direction of the applied load). Therefore, the ratio of y_{max} to Δ is

$$\frac{y_{max}}{\Delta} = \frac{0.2}{0.52} = 0.38 \quad (46)$$

From Figure 5 with l_u/l_c equal to 0, the length of frictional resistance to deduct is about

$$l_n = 0.45\,l_c = 0.45(17.6) = 7.9 \text{ ft} \quad (47)$$

Because 8 ft of frictional resistance within the predrilled hole has already been neglected, an additional deduction is not necessary, resulting in an allowable vertical capacity, P, of the pile for Load Group IV of

$$P = [(0.8)(8) + (1.2)(16)]1.25 = 32 \text{ tons} \quad (48)$$

which is greater than the applied load of 59 kips. Therefore, the pile length established from the preliminary design (Equation 13) is adequate for Case B. [Note that Case B was not con-

trolled by the thermal movement of the abutment (Load Group IV) but was controlled by the gravity load (Load Group I)].

Case C Capacity

The horizontal displacement of the pile head does not affect the capacity of the soil to support the load (Case C). Because the spacing of the piles (6 ft-4 in. center-to-center) is greater than three times the pile dimension, Case C capacity is adequate.

SUMMARY AND CONCLUSIONS

Pile ductility affects the ultimate strength and behavior of piles subjected to combined lateral displacement and vertical load. Based on the moment-rotation capacity of a pile, two approaches to determine the capacity of the pile as a structural member (Case A) were presented. Alternative 1 is an elastic design approach that should be applied for piles with limited ductility such as timber, concrete, and steel piles without inelastic rotation capabilities. For this alternative, all stresses induced by the lateral displacement of the pile head and gravity loads are considered in the design. When sufficient pile ductility exists, Alternative 2 is a design approach that can be applied to recognize redistribution of internal forces caused by plastic hinge rotation. For this alternative, the first-order stresses, but not the strains, caused by thermally induced lateral displacement of the pile head are neglected. These displacement-induced bending stresses do not affect the ultimate strength of the pile when the moment-rotation capacity exceeds the moment-rotation demand. The pile strains are investigated indirectly by a ductility criterion that was presented in terms of the pile head displacement.

To illustrate the two design alternatives, a pile design example for an integral abutment was presented. The design for a fixed-headed, HP-shaped, friction pile was simplified by the use of nondimensional graphs for equivalent cantilever lengths and effective friction length loss. The example showed that according to Alternative 1, the pile had insufficient capacity. However, according to Alternative 2, the pile had sufficient ductility, even though the pile was not a compact section and had adequate strength. For the example presented, Case B requirements, involving AASHTO Group I loading, controlled the pile design when Alternative 2 was applied for Case A conditions. The integral abutment lateral displacement, caused by a thermal expansion and contraction of 0.52 in. for the 360-ft bridge, did not detract from the strength of the pile. In fact, the lateral displacement of the pile head could have been as large as 1.14 in. before the integral abutment design would have detracted from the allowable pile load, indicating that this bridge could have been about twice as long. By recognizing the ductility characteristics of piles, Alternative 2 will permit the safe design of integral abutment bridges that can be significantly longer than those designed according to Alternative 1.

ACKNOWLEDGMENTS

The research presented in this paper was conducted by the Engineering Research Institute of Iowa State University and was sponsored by the Iowa Department of Transportation (Iowa DOT), Highway Division, through the Iowa Highway Research Board. The authors wish to express their appreciation to graduate students Patrick Ebner, Douglas Johnson, and Xiaohuan Lu, who assisted in the research efforts. Iowa DOT Engineers William Lundquist, Henry Gee, and John Harkin made valuable suggestions with regard to some of the design criteria.

REFERENCES

1. W. Zuk. *Jointless Bridges*, Report VHTRC-81-R48; FHWA/VA-81/48. Virginia Highway and Transportation Research Council, Springfield; FHWA, U.S. Department of Transportation, June 1981.
2. A. M. Wolde-Tinsae, L. F. Greimann, and P.-S. Yang. *Nonlinear Pile Behavior in Integral Abutment Bridges*. Project HR-227, ISU-ERI-Ames 82123. Iowa Department of Transportation, Des Moines, Feb. 1982.
3. A. M. Wolde-Tinsae, J. E. Klinger, M. Mafi, P. Albrecht, J. White, and N. Buresli. *Performance and Design of Jointless Bridges*. Contract DTFH61-85-C-00092, Final Report. Department of Civil Engineering, University of Maryland; FHWA, U.S. Department of Transportation, June 1987.
4. D. L. Allen. *A Survey of the States on Problems Related to Bridge Approaches*. Final Report UKTRP-85-25. Transportation Research Program, College of Engineering, University of Kentucky, Lexington; FHWA, U.S. Department of Transportation, Oct. 1985.
5. L. F. Greimann, R. E. Abendroth, D. E. Johnson, and P. E. Ebner. *Pile Design and Tests for Integral Abutment Bridges*. Project HR-273, ISU-ERI-Ames 88060, Final Report. Iowa Department of Transportation, Des Moines, Dec. 1987.
6. L. F. Greimann, P.-S. Yang, and A. M. Wolde-Tinsae. Nonlinear Analysis of Integral Abutment Bridges. *Journal of Structural Engineering*, ASCE, Vol. 112, No. 10, Oct. 1986, pp. 2263–2280.
7. L. F. Greimann and A. M. Wolde-Tinsae. Design Models for Piles in Jointless Bridges. *Journal of Structural Engineering*, ASCE, Vol. 114, No. 6, June 1988, pp. 1354–1371.
8. M. T. Davisson and K. E. Robinson. Bending and Buckling of Partially Embedded Piles. *Proc., 6th International Conference on Soil Mechanics and Foundation Engineering*, Montreal, Canada, Vol. 2, 1965, pp. 243–246.
9. H. G. Poulos and E. H. Davis. *Pile Foundation Analysis and Design*. John Wiley & Sons, Inc., New York, 1980.
10. B. G. Neal. *The Plastic Methods of Structural Analysis*. 2nd ed. John Wiley & Sons, Inc., New York, 1963.
11. M. R. Horn. *Plastic Theory of Structures*. Massachusetts Institute of Technology Press, Cambridge, 1971.
12. *Manual of Steel Construction*, 8th ed. American Institute of Steel Construction, Chicago, Ill., 1980.
13. T. V. Galambos and M. G. Lay. Studies of the Ductility of Steel Structures. *Journal of Structural Engineering*, ASCE, Vol. 91, No. 8, Aug. 1965. pp. 125–151.
14. M. G. Lay. Flange Local Buckling in Wide-Flange Shapes. *Journal of Structural Engineering*, ASCE, Vol. 91, No. 12, Dec. 1965, pp. 95–116.
15. M. G. Lay and T. V. Galambos. Inelastic Beams Under Moment Gradient. *Journal of Structural Engineering*, ASCE, Vol. 93, No. 2, Feb. 1967, pp. 381–399.
16. A. F. Lukey and P. F. Adams. Rotation Capacity of Beams Under Moment Gradient. *Journal of Structural Engineering*, ASCE, Vol. 95, No. 6, June 1969, pp. 1173–1188.
17. *Manual of Steel Construction: LRFD*, 1st ed., American Institute of Steel Construction, Chicago, Ill., 1986.
18. W. G. Fleming, A. J. Weltman, M. F. Randolph, and W. K. Elson. *Piling Engineering*. Halsted Press, New York, 1985.
19. M. G. Spangler. *Soil Engineering*, 2nd ed., International Textbook Company, 1960.

Publication of this paper sponsored by Committee on General Structures.